although our work does not allow us to make an estimate of the magnitude of this parameter. For poly[dGdC], the rate of reverse transfer ($k = 3.3 \times 10^{10}$ s^{-1}; $\Delta G° = -146$ kJ mol^{-1}) is significantly slower than that of the forward reaction ($k = 2.5 \times 10^{11}$ s^{-1}; $\Delta G° = -76$ kJ mol^{-1}) despite its higher thermodynamic driving force. This cannot be taken to indicate that the reverse reaction falls within the Marcus "inverted region", however, since the forward and reverse steps may display quite distinct rate vs driving force profiles.[48] Further studies are needed before we can estimate the reorganization energy for a polynucleotide matrix, and we are attempting to evaluate this important parameter by using a series of intercalators of similar structure but differing reduction potential.

Acknowledgment. We thank P. T. Snowden for providing specialized software for data analysis and the U.S. Department of Energy for providing a grant enabling construction of the femtosecond laser flash spectrograph. This work was supported by the National Science Foundation (CHE 9102657). The CFKR is supported jointly by the Biotechnology Research Resources Division of the NIH (RR00886) and by The University of Texas at Austin.

(48) Zou, C.; Miers, J. B.; Ballew, R. M.; Diott, D. D.; Schuster, G. B. *J. Am. Chem. Soc.* **1991**, *113*, 7823.

Crystal Structure and Magnetic Properties of $[Ln_2Cu_4]$ Hexanuclear Clusters (where Ln = trivalent lanthanide). Mechanism of the Gd(III)–Cu(II) Magnetic Interaction

Marius Andruh,† Isabelle Ramade,† Epiphane Codjovi,† Olivier Guillou,† Olivier Kahn,*,† and Jean Christian Trombe‡

Contribution from the Laboratoire de Chimie Inorganique, URA 420, Université de Paris Sud, 91405 Orsay, France, and CEMES-LOE, UPR 8011, PO Box 4337, 31055 Toulouse, France.
Received July 31, 1992

Abstract: The hexanuclear clusters $[Ln_2Cu_4(fsaaep)_4(NO_3)_6]\cdot 0.5(CH_3OH\cdot H_2O)$ (abbreviated as $[Ln_2Cu_4]$) have been synthesized; Ln is a trivalent lanthanide and $(fsaaep)^{2-}$ is the ligand deriving from 3-(*N*-2-(pyridylethyl)formimidoyl)salicylic acid. The crystal structure of the compound with Ln = Pr has been solved. This compound crystallizes in the orthorhombic system, space group $P2_12_12_1$. The lattice parameters are $a = 18.746(4)$ Å, $b = 24.196(4)$ Å, $c = 17.053(4)$ Å, and $Z = 4$. The structure consists of $[Pr_2Cu_4]$ entities in which the metal ions form a chair-shaped hexagon. The two praseodymium atoms are located on both sides of a double layer containing the four copper atoms. The copper environments are elongated distorted octahedra, and the praseodymium environments are bicapped square antiprisms. The magnetic susceptibility and the magnetization of $[La_2Cu_4]$ and $[Gd_2Cu_4]$ have been investigated. As far as the magnetic properties are concerned, the hexanuclear clusters may be viewed as two independent Cu(II)Ln(III)Cu(II) triads. The magnetic susceptibility data for $[La_2Cu_4]$ have revealed a weak Cu(II)–Cu(II) interaction through the closed-shell rare earth ion characterized by the interaction parameter $J_{CuCu} = -3.13$ cm^{-1} (the interaction Hamiltonian being of the form $H = -JS_A\cdot S_B$). The magnetic susceptibility data for $[Gd_2Cu_4]$ have shown that the ground-state spin for the Cu(II)Gd(III)Cu(II) triad is $S = {}^9/_2$; the Gd(III)–Cu(II) interaction is ferromagnetic with an interaction parameter $J_{GdCu} = 6.0$ cm^{-1}. The field dependence of the magnetization measured at both 2 and 30 K confirms the nature of the ground state and of the Gd(III)–Cu(II) interaction. The heart of the paper is devoted to the mechanism of the Gd(III)–Cu(II) interaction. The ferromagnetic nature of this interaction is attributed to the coupling between the Gd(III)Cu(II) ground configuration and the Gd(II)Cu(III) charge-transfer excited configuration in which an electron is transferred from the singly-occupied 3d-type copper orbital toward an empty 5d-type gadolinium orbital. A semiquantitative estimate of J_{GdCu} is performed which agrees fairly well with the value deduced from the magnetic data. It is emphasized that the Gd(III)–Cu(II) interaction is quite peculiar in the sense that owing to the contraction of the 4f orbitals the usual mechanisms involving 4f–3d overlap densities are inoperative.

Introduction

In the past two decades or so, a large number of heteropolymetallic compounds have been described. The studies of these compounds have often been performed either in relation to the modeling of some metalloenzymes containing several kinds of metal ions or with the perspective to design novel molecular materials, in particular molecular-based magnets. A particular emphasis has been brought to the magnetic properties.[1] The main idea emerging from those studies is that the interaction between two nonequivalent magnetic centers may lead to situations which cannot be encountered with species containing a unique kind of spin carrier. In fact, the recent investigation of the magnetic properties of heteropolymetallic compounds has represented quite an important contribution to the development of molecular ferromagnetism as a whole[2] and has allowed the introduction of several important new concepts: (i) the importance of the relative symmetries of the interacting magnetic orbitals;[3,4] (ii) the strict orthogonality of the magnetic orbitals favoring the stabilization of the state of highest spin;[3,5-7] (iii) the irregular spin-state structure leading to molecular systems with a high spin in the ground state despite antiferromagnetic interactions between nearest

†Université de Paris Sud.
‡CEMES-LOE.

(1) Kahn, O. *Struct. Bonding (Berlin)* **1987**, *68*, 89.
(2) Kahn, O. *Molecular Magnetism*; Verlag-Chemie: New York, in press.
(3) Kahn, O.; Galy, J.; Journaux, Y.; Jaud, J.; Morgenstern-Badarau, I. *J. Am. Chem. Soc.* **1982**, *104*, 2165.
(4) Journaux, Y.; Kahn, O.; Zarembowitch, J.; Galy, J.; Jaud, J. *J. Am. Chem. Soc.* **1983**, *105*, 7585.
(5) Kahn, O.; Prins, R.; Reedijk, J.; Thompson, J. S. *Inorg. Chem.* **1987**, *26*, 3557.
(6) Benelli, C.; Dei, A.; Gatteschi, D.; Pardi, L. *Inorg. Chem.* **1988**, *27*, 2831.
(7) Caneschi, A.; Dei, A.; Gatteschi, D. *J. Chem. Soc., Chem. Commun.* **1992**, 630.

0002-7863/93/1515-1822$04.00/0

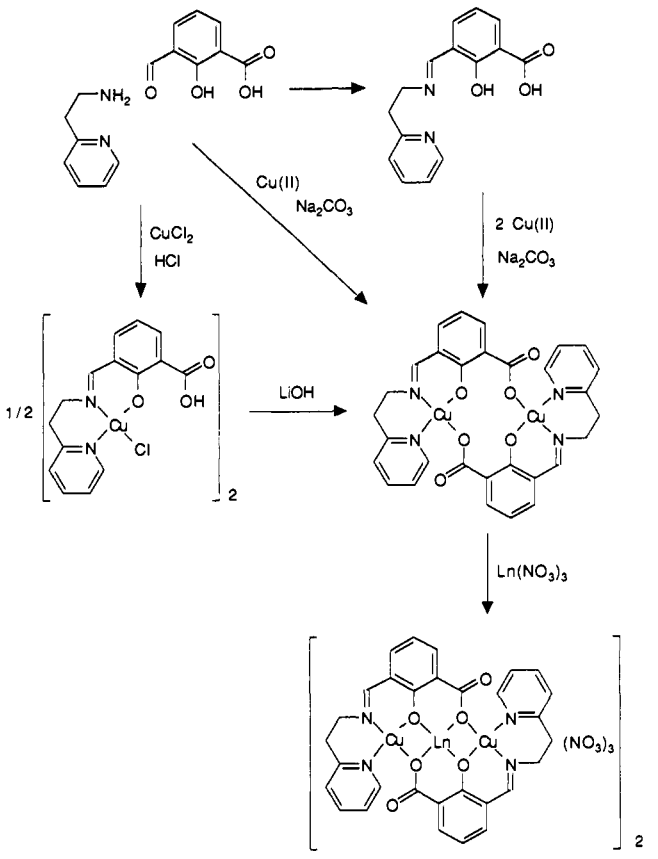

Figure 1. Schematic representation of the chemistry developed in this work.

neighbor ions;[8] (iv) the one-dimensional ferrimagnetism;[9–15] (v) the design of molecular-based magnets through crystal engineering of ferrimagnetic chain compounds;[16,17] and (vi) the peculiarity of the Gd(III)–Cu(II) interaction. This last point has been revealed by the pioneering work of Gatteschi and co-workers, who found that in a series of Cu(II)Gd(III)Cu(II) trinuclear compounds the Gd(III)–Cu(II) interaction was ferromagnetic, irrespective of the details of the molecular structure.[18–20] The same situation holds when Cu(II) is replaced by nitronyl nitroxide radicals.[21,22] The ferromagnetic nature of the Gd(III)–Cu(II) pair has been subsequently confirmed by Matsumoto, Okawa, and co-workers on a dinuclear compound[23,24] and then by us on one- and two-dimensional molecular materials.[25–27]

From the very beginning we have been most intrigued by the parallel spin alignment in the Gd(III)Cu(II) pair and have looked for its mechanism. This paper is devoted to this problem. First, we describe $[Ln_2Cu_4]$ hexanuclear clusters, where Ln is a trivalent lanthanide. The crystal structure has been solved for Ln = praseodymium. Next, we report on the magnetic susceptibility and magnetization of $[La_2Cu_4]$ and $[Gd_2Cu_4]$. From a magnetic point of view, these clusters behave as two independent Cu(II)-Ln(III)Cu(II) triads (Ln = La and Gd). The heart of the paper deals with the mechanism of the ferromagnetic interaction between Gd(III) and Cu(II). It is pointed out that the stabilization of the high-spin state arises from the coupling between the ground configuration and the excited configuration in which an electron is transferred from the singly-occupied 3d-type copper orbital toward an empty 5d-type gadolinium orbital. A semiquantitative estimate of the Gd(III)–Cu(II) interaction parameter is proposed which agrees fairly well with the experimental data and thus substantiates our mechanism.

Experimental Section

Syntheses. The chemistry developed in this work is schematized in Figure 1. 3-Formylsalicylic acid (H_2fsa) was prepared as previously reported.[28] $Ln(NO_3)_3 \cdot 6H_2O$ was prepared from Ln_2O_3 and HNO_3. The Schiff base 3-(*N*-(2-pyridylethyl)formimidoyl)salicylic acid (H_2fsaaep) was obtained by treating 2 mmol of H_2fsa with 2 mmol of 2-(2-aminoethyl)pyridine in 30 mL of ethanol. The resulting solution was refluxed for 15 min and then cooled at 4 °C. Yellow fibrous crystals were then obtained. ^{1}H-NMR ($CDCl_3$): δ 3.2 (t, 2 H), 4.2 (t, 2 H), 6.6 (t, 2 H), 7.3 (m, 3 H), 7.7 (t, 1 H), 8.1 (s, 1 H), 8.4 (d, 1 H), 8.7 (d, 1 H), 14 (br s, 1 H), 15.9 (br s, 1 H). The copper(II) chloro-bridged dimer $[Cu(Hfsaaep)Cl]_2$ was prepared by a template procedure as follows: 1 mmol of 2-(2-aminoethyl)pyridine was added to 1 mmol of H_2fsa. To the mixture were successively added 1.5 mL of a 37% HCl aqueous solution and 1 mmol of copper(II) chloride dihydrate. The mixture was stirred, and the resulting green precipitate was filtered off. Single crystals of $[Cu(Hfsaaep)Cl]_2$ were obtained by slow evaporation from a 50/50 methanol–acetonitrile mixture. The compound $[Cu(fsaaep)]_2 \cdot 5H_2O$ is the precursor of the $[Ln_2Cu_4(fsaaep)_4(NO_3)_6]$ entities. This precursor may be obtained by one of the three following routes: (i) by treating the ligand itself, H_2fsaaep, in a Na_2CO_3 or LiOH aqueous solution with a copper(II) salt; (ii) by treating the chloro-bridged dimer $[Cu(Hfsaaep)Cl]_2$ with a LiOH aqueous solution; or (iii) by a template procedure. This method is the most direct and therefore the most suitable. To an aqueous solution (60 mL) containing 2 mmol of H_2fsa and 212 mg of sodium carbonate was added 2 mmol of 2-(2-aminoethyl)-pyridine with stirring at room temperature. After 15 min, an aqueous solution (50 mL) containing 1.8 mmol of copper(II) perchlorate was added very slowly with stirring. The resulting mixture was stirred further for 1 h, and then the blue-grayish precipitate of $[Cu(fsaaep)]_2 \cdot 5H_2O$ was filtered off, washed with water, and dried under vacuum. Any attempt to obtain single crystals of $[Cu(fsaaep)]_2 \cdot 5H_2O$ failed. Anal. Calcd for $C_{30}H_{34}N_4O_{11}Cu_2$: C, 47.77; H, 4.50; N, 7.42; Cu, 16.97. Found: C, 47.17; H, 4.35; N, 7.23; Cu, 16.64. In a general procedure, the $[Ln_2Cu_4(fsaaep)_4(NO_3)_6]_2$ compounds were synthesized as follows: to a suspension of 1 mmol of $[Cu(fsaaep)]_2 \cdot 5H_2O$ in 20 mL of acetonitrile was added with stirring a solution of 1 mmol of $Ln(NO_3)_3 \cdot 6H_2O$ in 15 mL of acetonitrile. The resulting mixture was stirred for 3 h at room temperature. The green microcrystals of $[Ln_2Cu_4(fsaaep)_2(NO_3)_6]$ were collected by suction filtration. Single crystals of $[Pr_2Cu_4(fsaaep)_4(NO_3)_6]_2 \cdot 0.5(CH_3OH \cdot H_2O)$ were obtained by slow diffusion of acetonitrile in the methanolic solution of the compound.

Crystallographic Data Collection and Structure Determination. A 0.8 × 0.4 × 0.05-mm^3 platelike single crystal limited by the (010), (011), and (111) faces was mounted on an CAD4 Enraf–Nonius computer-controlled X-ray diffractometer. Orientation matrices and accurate unit cell constants were derived from a least-squares refinement of the setting

(8) Pei, Y.; Journaux, Y.; Kahn, O. *Inorg. Chem.* **1988**, *27*, 399.
(9) Verdaguer, M.; Julve, M.; Michalowicz, A.; Kahn, O. *Inorg. Chem.* **1983**, *22*, 2624.
(10) Gleizes, A.; Verdaguer, M. *J. Am. Chem. Soc.* **1984**, *106*, 3727.
(11) Pei, Y.; Sletten, J.; Kahn, O. *J. Am. Chem. Soc.* **1986**, *108*, 3143.
(12) Pei, Y.; Verdaguer, M.; Kahn, O.; Sletten, J.; Renard, J. P. *Inorg. Chem.* **1987**, *26*, 138.
(13) Beltran, D.; Escriva, E.; Drillon, M. *J. Chem. Soc., Faraday Trans.* **1982**, *78*, 1773.
(14) Drillon, M.; Coronado, E.; Beltran, D.; Georges, R. *J. Appl. Phys.* **1984**, *57*, 3353.
(15) Drillon, M.; Coronado, E.; Georges, R.; Ganduzzo, J. C.; Curely, J. *Phys. Rev. B* **1989**, *40*, 10992.
(16) Kahn, O.; Pei, Y.; Verdaguer, M.; Renard, J. P.; Sletten, J. *J. Am. Chem. Soc.* **1988**, *110*, 782.
(17) Nakatani, K.; Carriat, J. Y.; Journaux, Y.; Kahn, O.; Lioret, F.; Renard, J. P.; Pei, Y.; Sletten, J.; Verdaguer, M. *J. Am. Chem. Soc.* **1989**, *111*, 5739.
(18) Bencini, A.; Benelli, C.; Caneschi, A.; Carlin, R. L.; Dei, A.; Gatteschi, D. *J. Am. Chem. Soc.* **1985**, *107*, 8128.
(19) Bencini, A.; Benelli, C.; Caneschi, A.; Dei, A.; Gatteschi, D. *Inorg. Chem.* **1986**, *25*, 572.
(20) Benelli, C.; Caneschi, A.; Gatteschi, D.; Guillou, O.; Pardi, L. *Inorg. Chem.* **1990**, *29*, 1751.
(21) Benelli, C.; Caneschi, A.; Gatteschi, D.; Pardi, L.; Rey, P.; Shum, D. P.; Carlin, R. L. *Inorg. Chem.* **1989**, *28*, 272.
(22) Benelli, C.; Caneschi, A.; Fabretti, A. C.; Gatteschi, D.; Pardi, L. *Inorg. Chem.* **1990**, *29*, 4223.
(23) Matsumoto, N.; Sakamoto, M.; Tamaki, H.; Okawa, H.; Kida, S. *Chem. Lett.* **1989**, 853.
(24) Sakamoto, M.; Hashimura, M.; Matsuki, K.; Matsumoto, N.; Inoue, K.; Okawa, H. *Bull. Chem. Soc. Jpn.* **1991**, *64*, 3639.
(25) Guillou, O.; Bergerat, P.; Kahn, O.; Bakalbassis, E.; Boubekeur, K.; Batail, P.; Guillot, M. *Inorg. Chem.* **1992**, *31*, 110.
(26) Guillou, O.; Oushoorn, R. L.; Kahn, O.; Boubekeur, K.; Batail, P. *Angew. Chem., Int. Ed. Engl.* **1992**, *31*, 626.
(27) Guillou, O.; Kahn, O.; Oushoorn, R. L.; Boubekeur, K.; Batail, P. *Inorg. Chim. Acta* **1992**, *198–200*, 119.
(28) Duff, J. C.; Bills, E. J. *J. Chem. Soc.* **1932**, 1987.

Table I. Bond Lengths around the Metal Atoms for $[Pr_2Cu_4]$

atoms	distance (Å)	atoms	distance (Å)	atoms	distance (Å)	atoms	distance (Å)
Pr(1)–O(4)	2.44 (2)	Cu(2)–N(4)	1.96 (2)	Pr(1)–O(1)	2.45 (2)	Cu(2)–O(4)	1.95 (2)
Pr(1)–O(2)	2.50 (2)	Cu(2)–N(3)	2.01 (2)	Pr(1)–O(5)	2.48 (2)	Cu(2)–O(2)	2.05 (2)
Pr(1)–O(14)	2.52 (2)	Cu(2)–O(9)	2.34 (2)	Pr(1)–O(16)	2.59 (2)	Cu(2)–O(16)	2.63 (2)
Pr(1)–O(17)	2.59 (2)	Cu(3)–O(7)	1.95 (2)	Pr(1)–O(19)	2.60 (2)	Cu(3)–N(6)	1.99 (2)
Pr(1)–O(13)	2.62 (2)	Cu(3)–N(5)	2.01 (3)	Pr(1)–O(20)	2.63 (2)	Cu(3)–O(11)	2.07 (2)
Pr(2)–O(11)	2.46 (2)	Cu(3)–O(6)	2.32 (2)	Pr(2)–O(8)	2.44 (2)	Cu(3)–O(29)	2.61 (2)
Pr(2)–O(7)	2.48 (2)	Cu(4)–O(10)	1.93 (2)	Pr(2)–O(10)	2.45 (2)	Cu(4)–N(8)	1.96 (2)
Pr(2)–O(23)	2.51 (2)	Cu(4)–N(7)	1.99 (2)	Pr(2)–O(22)	2.58 (2)	Cu(4)–O(8)	2.01 (2)
Pr(2)–O(28)	2.58 (2)	Cu(4)–O(3)	2.29 (2)	Pr(2)–O(29)	2.59 (2)	Cu(4)–O(26)	2.72 (2)
Pr(2)–O(26)	2.63 (2)	Pr(1)–Cu(1)	3.428 (3)	Pr(2)–O(25)	2.61 (2)	Pr(1)–Cu(2)	3.418 (3)
Cu(1)–O(1)	1.95 (2)	Pr(2)–Cu(3)	3.400 (3)	Cu(1)–N(2)	1.97 (2)	Pr(2)–Cu(4)	3.426 (3)
Cu(1)–O(5)	2.00 (2)	Cu(1)–Cu(2)	5.886 (4)	Cu(1)–N(1)	2.07 (2)	Cu(3)–Cu(4)	5.855 (4)
Cu(1)–O(12)	2.31 (2)	Cu(1)–Cu(3)	4.596 (4)	Cu(1)–O(20)	2.65 (2)	Cu(2)–Cu(4)	4.702 (4)

angles of 25 reflections with θ between 8.2 and 17°. During the data collection a decay of a standard reflection intensity of 10% and a widening (mean value for the 25 reflections around 15%) were observed. A possible explanation of these phenomena will be discussed below. The data were corrected for this decay, for Lorentz and polarization effects, and for absorption using the DIFABS program.[29] Structure determination was refined applying full-matrix least-squares techniques on an Alliant VF1X/80 computer using programs listed in ref 30. Atomic scattering factors were taken from ref 31. Throughout the refinement the minimized function was $\sum w(F_o - |F_c|)^2$, where F_o and $|F_c|$ are the observed and calculated structure factor amplitudes, respectively. The compound crystallizes in the orthorhombic system, space group $P2_12_12_1$, with a = 18.746(4), b = 24.196(4), and c = 17.053(4) Å. Two independent praseodymium atoms per asymmetric unit were localized from the Patterson map. The other atoms appeared from successive Fourier or difference Fourier techniques. At this point, some residual peaks were assigned to one methanol and one water molecule, with a 50% site occupancy. The hydrogen atoms were introduced in the last cycles of refinement as fixed contributors. Only metal atoms were refined anisotropically. Due to a noncentrosymmetric space group, the two enantiomorph forms were tested; the reliability factor difference was about 0.005. The final cycle of refinement, based on 4250 reflections with $I > 3\sigma(I)$ and 483 variables, converged with unweighted and weighted agreement factors R = 0.071 and R_w = 0.087; the largest parameter shift was 0.013 in esd. The deviation in the observed unit weight was 2.3. Maximum peaks in the final difference Fourier map ranged from 2.3 to 1.4 e Å^{-3} for metal atoms and 1 e Å^{-3} for other reflections. The interatomic distances and angles around the metal atoms and the nitrato ions are given in Tables I and II, respectively. The $[La_2Cu_4]$ and $[Gd_2Cu_4]$ compounds were found to be isomorphous with $[Pr_2Cu_4]$.

Magnetic Measurements. The magnetic susceptibility measurements were carried out with two apparatus: (i) a Faraday-type magnetometer working down to 4.2 K and (ii) a SQUID magnetometer working down to 1.8 K in both the low-field and the high-field (up to 8 T) regimes. The magnetization measurements were carried out with the SQUID magnetometer.

EPR Spectra. The X-band powder EPR spectra were recorded at various temperatures with a ER 200 Bruker spectrometer equipped with a helium continuous-flow cryostat and a Hall probe.

Description of the Structure of $[Pr_2Cu_4]$

The unit cell contains four discrete entities of $[Pr_2Cu_4(fsaaep)_4(NO_3)_6]$ (hereafter abbreviated as $[Pr_2Cu_4]$) and intervening disordered water and methanol molecules. A simplified view of $[Pr_2Cu_4]$ is shown in Figure 2. The six metal atoms form a chair-shaped hexagon, with the distances shown in Figure 3. The Pr1Pr2Cu1Cu2 atoms on the one hand and the Pr1Pr2Cu3Cu4 atoms on the other hand form almost perfect planes.

The two praseodymium atoms are located of both sides of a double layer containing the four copper atoms; Cu1 and Cu2 and their respective equatorial positions are located in one of the layers, and Cu3 and Cu4 are in the other. The mean planes of these layers make a dihedral angle of 1.8(6)°, and the distance between these layers is about 3.95 Å. The distances of the Pr1 and Pr2 atoms from the neighboring layer are equivalent, 1.73 Å. The dihedral angle between the planes Cu1Pr1Cu2 and Cu3Pr2Cu4 is equal to 54.6(4)°. Although there is no symmetry element within $[Pr_2Cu_4]$, this hexanuclear entity may be viewed as a pair of heterotrinuclear units. The copper atoms belonging to two $PrCu_2$ units are bridged two-by-two by carboxylato groups, with Cu–O short bonds in the copper basal planes (average distance 1.9 Å) and Cu–O long bonds involving oxygen atoms occupying the apical positions (average distance, 2.32(2) Å). Within a trinuclear unit, each praseodymium atom is bridged to two copper atoms through one carboxylic and one phenolic oxygen atom. The Pr–Cu distances range from 3.400(3) to 3.428(3) Å. The Pr–O–Cu bridging angles range from 97.1(6) to 102.2(7)°.

The copper environments may be considered as elongated distorted octahedra (see Figure S1[46]). The equatorial positions are occupied by two nitrogen and two oxygen atoms, with Cu–N and Cu–O bond lengths ranging from 1.96(2) to 2.07(2) Å. One of the apical positions is occupied by the oxygen atom of the carboxylic group involved in the bridges between the layers with

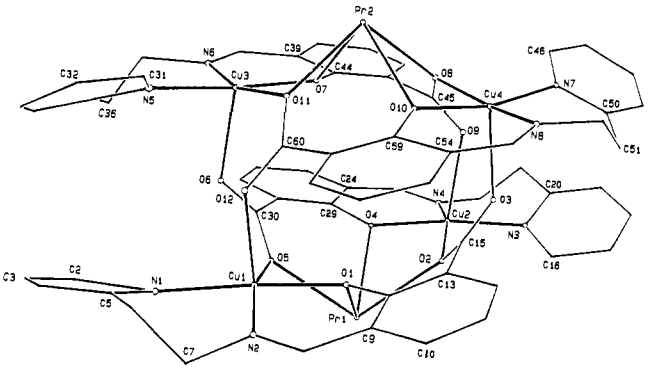

Figure 2. View of the $[Pr_2Cu_4]$ entity along with the atomic labeling scheme. For a sake of clarity, the nitrato ions chelated to the praseodymium atoms are not represented.

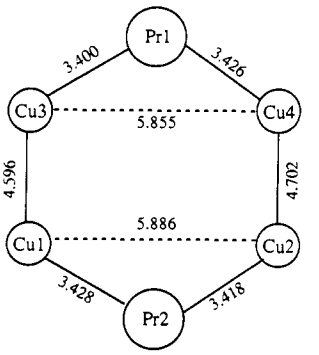

Figure 3. Intermetallic distances (Å) in the Pr_2Cu_4 hexagon.

(29) Walker, N.; Stuart, D. *Acta Crystallogr. Sect. A* **1983**, *33*, 158.
(30) Sheldrick, G. M. *SHELX, Program for Crystal Structure determination*; University of Cambridge, England, 1976.
(31) *International Tables for X-ray Crystallography*; Kynoch Press: Birmingham, 1974; Vol. 4, Tables 2.2.A and 2.3.1.

Table II. Bond Angles around the Metal Atoms for $[Pr_2Cu_4]$

atoms	angles (deg)	atoms	angles (deg)	atoms	angles (deg)	atoms	angles (deg)
O(4)-Pr(1)-O(1)	93.0 (5)	O(2)-Pr(1)-O(20)	134.2 (5)	N(1)-Cu(1)-O(12)	88.7 (7)	O(7)-Cu(3)-O(11)	78.3 (6)
O(4)-Pr(1)-O(5)	70.5 (5)	O(5)-Pr(1)-O(16)	142.7 (6)	O(12)-Cu(1)-O(20)	174.9 (6)	O(7)-Cu(3)-O(29)	83.2 (6)
O(4)-Pr(1)-O(16)	74.6 (6)	O(5)-Pr(1)-O(19)	71.1 (5)	N(4)-Cu(2)-N(3)	92.8 (8)	N(6)-Cu(3)-O(11)	164.5 (8)
O(4)-Pr(1)-O(19)	113.6 (5)	O(5)-Pr(1)-O(20)	70.9 (5)	N(4)-Cu(2)-O(9)	93.0 (8)	N(6)-Cu(3)-O(29)	95.6 (8)
O(4)-Pr(1)-O(20)	141.4 (5)	O(14)-Pr(1)-O(17)	113.6 (6)	O(4)-Cu(2)-N(3)	172.2 (7)	N(5)-Cu(3)-O(6)	89.4 (9)
O(1)-Pr(1)-O(5)	60.5 (5)	O(14)-Pr(1)-O(13)	49.2 (6)	O(4)-Cu(2)-O(9)	98.8 (6)	O(11)-Cu(3)-O(6)	103.3 (6)
O(1)-Pr(1)-O(16)	131.5 (5)	O(16)-Pr(1)-O(17)	48.8 (5)	N(3)-Cu(2)-O(2)	95.5 (7)	O(6)-Cu(3)-O(29)	175.5 (6)
O(1)-Pr(1)-O(19)	111.7 (5)	O(16)-Pr(1)-O(13)	70.2 (6)	O(8)-Pr(2)-O(29)	142.0 (5)	O(10)-Cu(4)-N(7)	166.3 (7)
O(1)-Pr(1)-O(20)	69.9 (5)	O(17)-Pr(1)-O(19)	68.5 (5)	O(8)-Pr(2)-O(25)	70.9 (6)	O(10)-Cu(4)-O(3)	100.2 (6)
O(2)-Pr(1)-O(14)	78.3 (6)	O(17)-Pr(1)-O(20)	115.5 (5)	O(7)-Pr(2)-O(23)	137.8 (6)	N(8)-Cu(4)-N(7)	94.5 (8)
O(2)-Pr(1)-O(17)	108.8 (5)	O(19)-Pr(1)-O(20)	49.7 (5)	O(7)-Pr(2)-O(28)	71.3 (6)	N(8)-Cu(4)-O(3)	92.7 (7)
O(2)-Pr(1)-O(13)	114.8 (6)	O(11)-Pr(2)-O(8)	103.7 (6)	O(7)-Pr(2)-O(26)	142.0 (6)	N(7)-Cu(4)-O(8)	94.6 (7)
O(5)-Pr(1)-O(14)	134.0 (5)	O(11)-Pr(2)-O(10)	69.3 (5)	O(10)-Pr(2)-O(23)	82.0 (6)	N(7)-Cu(4)-O(26)	92.1 (7)
O(5)-Pr(1)-O(17)	108.0 (5)	O(11)-Pr(2)-O(22)	118.8 (6)	O(10)-Pr(2)-O(28)	164.3 (6)	O(8)-Cu(4)-O(26)	77.5 (6)
O(5)-Pr(1)-O(13)	136.9 (6)	O(11)-Pr(2)-O(29)	67.7 (6)	O(10)-Pr(2)-O(26)	70.0 (6)	Pr(1)-O(1)-Cu(1)	101.6 (6)
O(14)-Pr(1)-O(16)	82.0 (6)	O(11)-Pr(2)-O(25)	173.2 (7)	O(23)-Pr(2)-O(22)	50.6 (7)	Pr(1)-O(2)-Cu(2)	97.0 (6)
O(14)-Pr(1)-O(19)	106.7 (6)	O(8)-Pr(2)-O(10)	60.8 (5)	O(23)-Pr(2)-O(29)	78.5 (6)	Pr(2)-O(7)-Cu(3)	99.7 (6)
O(14)-Pr(1)-O(20)	74.1 (6)	O(8)-Pr(2)-O(22)	135.9 (6)	O(23)-Pr(2)-O(25)	108.6 (7)	Pr(2)-O(8)-Cu(4)	100.2 (6)
O(16)-Pr(1)-O(19)	112.7 (6)	O(8)-Pr(2)-O(28)	105.9 (6)	O(22)-Pr(2)-O(29)	70.9 (6)	O(2)-Cu(2)-O(9)	102.7 (6)
O(16)-Pr(1)-O(20)	141.5 (5)	O(8)-Pr(2)-O(26)	73.0 (6)	O(22)-Pr(2)-O(25)	67.4 (7)	O(9)-Cu(2)-O(16)	173.9 (6)
O(17)-Pr(1)-O(13)	71.2 (6)	O(7)-Pr(2)-O(10)	95.1 (5)	O(28)-Pr(2)-O(26)	115.9 (6)	O(7)-Cu(3)-N(5)	171.0 (8)
O(19)-Pr(1)-O(13)	68.9 (6)	O(7)-Pr(2)-O(22)	140.6 (6)	O(29)-Pr(2)-O(26)	140.3 (6)	O(7)-Cu(3)-O(6)	98.5 (6)
O(13)-Pr(1)-O(20)	71.3 (5)	O(7)-Pr(2)-O(29)	74.6 (5)	O(26)-Pr(2)-O(25)	49.2 (6)	N(6)-Cu(3)-N(5)	94.2 (9)
O(11)-Pr(2)-O(7)	61.9 (5)	O(7)-Pr(2)-O(25)	111.7 (6)	O(1)-Cu(1)-O(5)	77.9 (6)	N(6)-Cu(3)-O(6)	88.6 (8)
O(11)-Pr(2)-O(23)	78.1 (6)	O(10)-Pr(2)-O(22)	122.8 (6)	O(1)-Cu(1)-O(12)	98.4 (7)	N(5)-Cu(3)-O(11)	95.9 (8)
O(11)-Pr(2)-O(28)	109.0 (6)	O(10)-Pr(2)-O(29)	135.4 (6)	N(2)-Cu(1)-O(5)	161.5 (8)	N(5)-Cu(3)-O(29)	88.6 (6)
O(11)-Pr(2)-O(26)	134.1 (6)	O(10)-Pr(2)-O(25)	110.4 (6)	N(2)-Cu(1)-O(12)	92.0 (8)	O(11)-Cu(3)-O(29)	72.9 (6)
O(8)-Pr(2)-O(7)	69.3 (5)	O(23)-Pr(2)-O(28)	113.3 (7)	O(5)-Cu(1)-N(1)	94.5 (7)	O(10)-Cu(4)-N(8)	91.2 (7)
O(8)-Pr(2)-O(23)	137.8 (6)	O(23)-Pr(2)-O(26)	76.3 (7)	O(5)-Cu(1)-O(20)	78.0 (6)	O(10)-Cu(4)-O(8)	77.6 (6)
O(4)-Pr(1)-O(2)	61.3 (5)	O(22)-Pr(2)-O(28)	72.2 (7)	N(1)-Cu(1)-O(20)	96.1 (7)	O(10)-Cu(4)-O(26)	75.4 (6)
O(4)-Pr(1)-O(14)	138.6 (5)	O(22)-Pr(2)-O(26)	69.3 (6)	N(4)-Cu(2)-O(4)	92.5 (7)	N(8)-Cu(4)-O(8)	165.5 (8)
O(4)-Pr(1)-O(17)	74.8 (5)	O(28)-Pr(2)-O(29)	49.8 (6)	N(4)-Cu(2)-O(2)	163.2 (8)	N(8)-Cu(4)-O(26)	90.9 (7)
O(4)-Pr(1)-O(13)	141.8 (6)	O(28)-Pr(2)-O(25)	69.3 (7)	N(4)-Cu(2)-O(16)	93.0 (7)	N(7)-Cu(4)-O(3)	92.0 (7)
O(1)-Pr(1)-O(2)	69.8 (5)	O(29)-Pr(2)-O(25)	113.7 (7)	O(4)-Cu(2)-O(2)	78.0 (6)	O(8)-Cu(4)-O(3)	98.2 (6)
O(1)-Pr(1)-O(14)	80.0 (5)	O(1)-Cu(1)-N(2)	90.4 (8)	O(4)-Cu(2)-O(16)	82.1 (6)	O(3)-Cu(4)-O(26)	174.4 (6)
O(1)-Pr(1)-O(17)	166.1 (5)	O(1)-Cu(1)-N(1)	170.6 (7)	N(3)-Cu(2)-O(9)	86.8 (7)	Pr(1)-O(5)-Cu(1)	99.5 (6)
O(1)-Pr(1)-O(13)	122.4 (6)	O(1)-Cu(1)-O(20)	77.0 (6)	N(3)-Cu(2)-O(16)	91.8 (7)	Pr(1)-O(4)-Cu(2)	101.7 (6)
O(2)-Pr(1)-O(5)	106.3 (5)	N(2)-Cu(1)-N(1)	95.5 (8)	O(2)-Cu(2)-O(16)	72.1 (6)	Pr(2)-O(11)-Cu(3)	97.1 (6)
O(2)-Pr(1)-O(16)	66.5 (6)	N(2)-Cu(1)-O(20)	85.6 (7)	O(7)-Cu(3)-N(6)	90.2 (8)	Pr(1)-O(10)-Cu(4)	102.2 (7)
O(2)-Pr(1)-O(19)	174.9 (5)	O(5)-Cu(1)-O(12)	103.6 (6)				

an average Cu–O bond length of 2.32(2) Å. The other apical position (seen in Figure 4 but not in Figure 2) is occupied by an oxygen atom belonging to a nitrato ion already linked to a rare earth atom. The Cu–O apical bond lengths of this kind range from 2.61(2) to 2.72(2) Å. The copper atoms are pulled out of the equatorial planes toward the closest apical positions (O12, O9, O6, O3) by an average value of 0.18 Å. However, the two copper atoms and the eight equatorial positions are close to a plane, the atom-to-mean plane distances not exceeding 0.09 Å for Cu1 and Cu2, 0.03 Å for Cu3, and 0.01 Å for Cu4.

In addition to the oxygen atoms belonging to the $(fsaaep)^{2-}$ ligands, the rare earth atoms achieve their environment with six oxygen atoms coming from three bidentate nitrato ions, as shown in Figure 4. The average value of the Pr–O bond lengths involving nitrato groups (2.59(2) Å) is significantly longer than that involving the $(fsaaep)^{2-}$ ligands (2.47(2) Å). The coordination polyhedron around the praseodymium atom may be described as a bicapped square antiprism, the capping positions around Pr1 being occupied by the atoms O2 and O19 (see Figure S2[46]). Due to the bidentate character of the NO_3^- ligands, their oxygen atoms from the "bite" are forced to be closer to each other (e.g., O13 to O14, O16 to O17, etc.), which provokes some distorsions of the polyhedron. Therefore, the basis O5O13O17O20 looks like a trapezoid. This basis makes a dihedral angle of 5.1(6)° with the other basis O1O4O14O16. The polyhedron around Pr2 is much the same: O11 and O25 occupy the capping positions, and O7O10O23O29 and O8O22O26O28 form the bases.

The nitrato groups play the role of bidentate ligands; four out of six are also linked to the copper atoms (see above). Interestingly, the two Pr–O bond lengths involving the same NO_3^- group are equal when the nitrato group is related to a copper atom

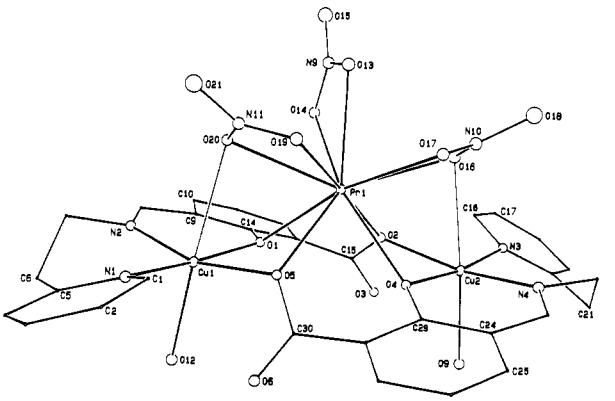

Figure 4. View of one of the $PrCu_2$ units showing the chelation of the nitrato ions toward the Pr1 atom.

(e.g., Pr1–O16 = Pr1–O17 = 2.59(2) Å) and different otherwise (e.g., Pr1–O13 = 2.62(2), Pr1–O14 = 2.52(2) Å). The nitrato groups are almost planar.

The geometry (bond lengths and angles) is not significantly different from one $(fsaaep)^{2-}$ ligand to another. The aromatic rings are roughly parallel two-to-two, which may contribute to strengthening the stability of $[Pr_2Cu_4]$ owing to π overlaps. In this respect the overlap is more pronounced between the phenolato rings than between the pyridine rings. It is more difficult to analyze the packing of the $[Pr_2Cu_4]$ entities within the lattice. Only one partial overlap can be found between the planes N5–C31 to C35 and $C54^i$ to $C59^i$ ($i = {}^1/_2 + x, {}^3/_2 + y, 2 - z$). C34 and C35 are distant from the mean plane of $C54^i$ to $C59^i$ by 3.4(2)

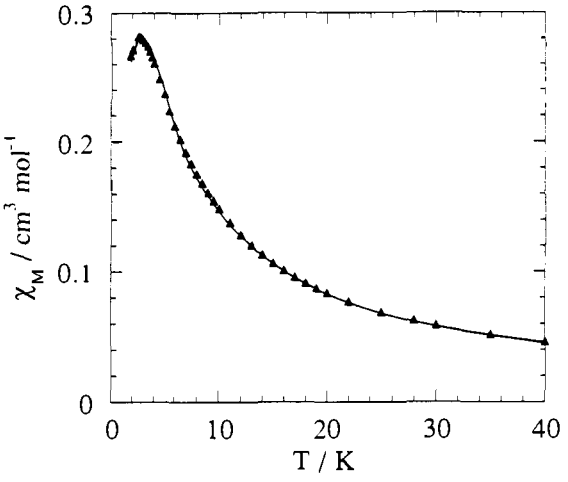

Figure 5. χ_M versus T plot for $[La_2Cu_4]$.

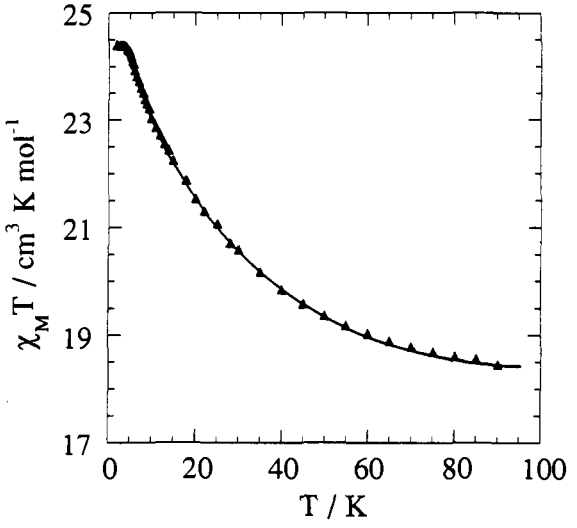

Figure 6. $\chi_M T$ versus T plot for $[Gd_2Cu_4]$.

and 3.7(2) Å, respectively. The solvent molecules apparently do not assume the lattice cohesion; their distances from the nitrato oxygen atoms are greater than 2.94(6) Å. A calculation of the potential solvent volume, i.e., the unoccupied area, leads to 10% of the unit cell volume.[32] Thus it may be assumed that some solvent is lost during the data collection, which would explain the decay of standard reflections and the widening of the reflection list.

Magnetic and EPR Properties

In this paper we focus on the magnetic properties of $[La_2Cu_4]$ and $[Gd_2Cu_4]$. In the former compound, the lanthanide ion La(III) is diamagnetic, and the magnetic study will provide some information about the interaction between the copper(II) ions. In the latter compound, Gd(III) has a $^8S_{7/2}$ free-ion ground state, without first-order angular momentum. The magnetic properties allow us to determine the nature and the magnitude of the Gd(III)–Cu(II) interaction.

$[La_2Cu_4]$. The χ_M versus T plot for $[La_2Cu_4]$ shown in Figure 5 presents a maximum at 2.55 K, which is characteristic of antiferromagnetic interactions between spin carriers, affording a diamagnetic ground state. The spin topology is that of a tetranuclear species (Cu1Cu2Cu3Cu4) with, in principle, both intralayer J_{CuCu} and interlayer J'_{CuCu} interaction parameters. In fact,

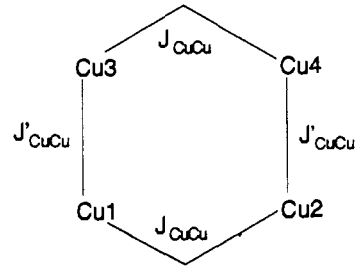

J'_{CuCu} may be expected to be negligibly small. Indeed, the spin density around a copper(II) ion in elongated octahedral surroundings is partially delocalized toward the four nearest neighbors in the equatorial plane and not toward the apical positions. The interlayer bridging network involves two such apical atoms (for instance, O6 and O12 between Cu1 and Cu2). The situation is quite reminiscent of what has been found in dissymmetric μ-1,3-azido copper(II) dimers, in which one terminal nitrogen atom of N_3^- occupies an equatorial position around a copper(II) ion with a short Cu–N distance and the other terminal nitrogen atom occupies an apical position around the other copper(II) ion with a long Cu–N distance. In such dimers the interaction parameter through the azido bridge is found to be 0.[33,34] Therefore, the antiferromagnetic interaction revealed by the magnetic susceptibility data occurs between copper(II) ions located within the same layer of either side of the La(III) ion. The two magnetic orbitals centered on Cu1 and Cu2 (or Cu3 and Cu4), respectively, are located in the same plane, such that they can interact in spite of the rather large Cu1···Cu2 separation (5.886 Å). The J_{CuCu} interaction parameter occurring in the spin Hamiltonian $-J_{CuCu}\mathbf{S}_{Cu1}\cdot\mathbf{S}_{Cu2}$ may then be obtained by a least-squares fit of the data of Figure 5 with the magnetic susceptibility equation valid for two independent copper(II) pairs. J_{CuCu} is found to be equal to -3.13 cm^{-1}. The agreement between observed and calculated χ_M values is then excellent, with $\sum[(\chi_M)^{obs} - (\chi_M)^{calc}]^2/\sum[(\chi_M)^{obs}]^2 = 1.1 \times 10^{-6}$. We will see below that the magnetic data for $[Gd_2Cu_4]$ confirm that the interlayer interaction parameter J'_{CuCu} is negligible.

$[Gd_2Cu_4]$. The magnetic susceptibility data for this compound are shown in Figure 6 in the form of the $\chi_M T$ versus T plot. $\chi_M T$ is equal to 17.5(1) cm^3 K mol^{-1} at room temperature (which corresponds to the value expected for the six uncoupled metal ions), remains practically constant down to ca. 100 K, increases regularly as the temperature is lowered further, and eventually reaches a plateau at very low temperatures with $\chi_M T = 24.4(1)$ cm^3 K mol^{-1}. Since the interlayer interaction parameter J'_{CuCu} is assumed to be negligible, the magnetic properties of $[Gd_2Cu_4]$ are similar to those of two independent Cu(II)Gd(III)Cu(II) triads. The energies $E(S,S')$ of low-lying states deduced from the interaction Hamiltonian

$$H = -J_{GdCu}\mathbf{S}_{Gd}\cdot(\mathbf{S}_{Cu1} + \mathbf{S}_{Cu2}) - J_{CuCu}\mathbf{S}_{Cu1}\cdot\mathbf{S}_{Cu2} \qquad (1)$$

are

$$E(^9/_2,1) = 0 \qquad E(^7/_2,1) = 9J_{GdCu}/2$$
$$E(^7/_2,0) = 7J_{GdCu}/2 + J_{CuCu} \qquad E(^5/_2,1) = 8J_{GdCu} \qquad (2)$$

J_{GdCu} is the Gd(III)–Cu(II) interaction parameter, and S and S' are the quantum numbers associated with the spin operators:

$$\mathbf{S} = \mathbf{S}' + \mathbf{S}_{Gd} \qquad \mathbf{S}' = \mathbf{S}_{Cu1} + \mathbf{S}_{Cu2} \qquad (3)$$

The curve of Figure 6 clearly reveals that the Gd(III)–Cu(II) interaction is ferromagnetic and that the ground state for the triad is $S = ^9/_2$, with the three local spins aligned in a parallel fashion.

(32) Spek, A. L. Vakgroep Algemeine Chemie, University of Utrecht, Afdeling Kristal-en Structururchemie, Padualann 8, Utrecht, The Netherlands, Platon-90, 1980–1990.

(33) Bkouche-Waksman, I.; Sikorav, S.; Kahn, O. J. *Crystallogr. Spectrosc. Res.* **1983**, *13*, 303.
(34) Charlot, M. F.; Kahn, O.; Chaillet, M.; Larrieu, C. *J. Am. Chem. Soc.* **1986**, *108*, 2574.
(35) Anderson, P. W. *Phys. Rev.* **1956**, *115*, 2.
(36) Anderson, P. W. In *Magnetism*; Rado, G. T., Suhl, H., Eds.; Academic Press: New York, 1963; Vol. 1, p 25.
(37) Briat, B.; Kahn, O. *J. Chem .Soc., Faraday Trans.* **1976**, *72*, 268.

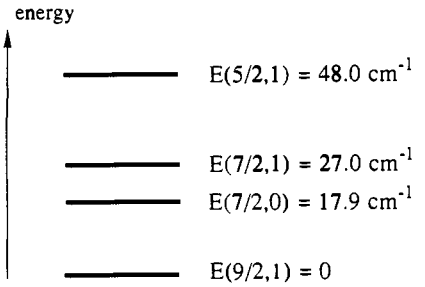

Figure 7. Energy spectrum for the low-lying states of the Cu(II)Gd(III)Cu(II) triad as deduced from the magnetic data for $[La_2Cu_4]$ and $[Gd_2Cu_4]$.

From the energies $E(S,S')$ and the equations relating local and molecular **g** tensors in a triad, it would be straightforward to express the magnetic susceptibility as a function of T and of four parameters, J_{GdCu}, J_{CuCu}, and the local Zeeman factors g_{Gd} and g_{Cu}. In fact, in order to avoid an overparametrization we imposed $J_{CuCu} = -3.13$ cm^{-1}, which is the value found in $[La_2Cu_4]$, and $g_{Gd} = g_{Cu} = g$. If so, J is found as 6.0 cm^{-1} and g as 1.99. The agreement factor expressed as $\sum[(\chi_M T)^{obs} - (\chi_M T)^{calc}]^2/\sum[(\chi_M T)^{obs}]^2$ is then equal to 1.3×10^{-4}. The spectrum of the low-lying states for the triad is represented in Figure 7.

Interestingly, we note that the presence of a plateau in the low-temperature range of the $\chi_M T$ versus T curve of Figure 6 justifies the assumption that J'_{CuCu} is negligible. Indeed, if it were not so, the two $S = {}^9/_2$ triad ground states would couple antiferromagnetically within the hexanuclear species and $\chi_M T$ for $[Gd_2Cu_4]$ would decrease as T tends to absolute 0. The constant value of $\chi_M T$ below ca. 5 K also indicates that the zero-field splitting within the ground state, if any, is much too small to be detected by the magnetic techniques.

To confirm the nature of the ground state, we investigated the variation of the magnetization M versus the field **H** at both 2 K and 30 K. At 2 K, only the ground state is significantly populated, and, as expected, the $M = f(\mathbf{H})$ curve closely follows the Brillouin function for two independent $S = {}^9/_2$ spins. On the other hand, at 30 K the excited states are significantly populated as well, and the magnetization curve is just between the Brillouin function for the six independent local spins and the Brillouin function for two independent $S = {}^9/_2$ triad spins, as shown in Figure 8 where M is expressed in $N\beta$ units and **H** in tesla.

We also investigated the X-band powder EPR spectra of $[La_2Cu_4]$ and $[Gd_2Cu_4]$. These spectra are not very informative. The former at any temperature above 4.2 K presents a single absorption at $g = 2.09$, without half-field transition, which indicates that the zero-field splitting within the triplet-pair state is too weak to be detected. The spectrum for $[Gd_2Cu_4]$ shows a very broad and symmetric absorption centered at $g = 2.00$ and a weak feature around 1000 G which might correspond to a forbidden transition within the $S = {}^9/_2$ triad ground state.

Why is the Gd(III)–Cu(II) Interaction Ferromagnetic?

Our findings concerning the nature of the Gd(III)–Cu(II) interaction confirm those of Gatteschi et al.[18-20] and Matsumoto et al.[23,24] What is remarkable is that the parallel spin alignment in the ground state does not depend on the details of the structure, which suggests that a rather general mechanism applies. In this section we will propose such a mechanism. We will consider a Gd(III)–Cu(II) pair, but the basic concepts could be easily extended to systems of higher nuclearity containing Gd(III)–Cu(II) motifs.

The peculiarity of the 4f singly-occupied orbitals of Gd(III) as compared to the 3d singly-occupied orbitals of first-row transition ions is their contraction around the nucleus and the fact that they are efficiently shielded by the 5s and 5p occupied orbitals. It follows that these 4f orbitals are extremely weakly delocalized toward the oxygen atoms surrounding the rare earth. As a consequence of this, the 4f-type magnetic orbitals of Gd(III) do not interact with the single 3d-type magnetic orbital of Cu(II). All integrals involving a 4f–3d overlap density vanish; the Heitler–London type interaction[2,38] between the ground states of Gd(III) and Cu(II) is therefore 0.

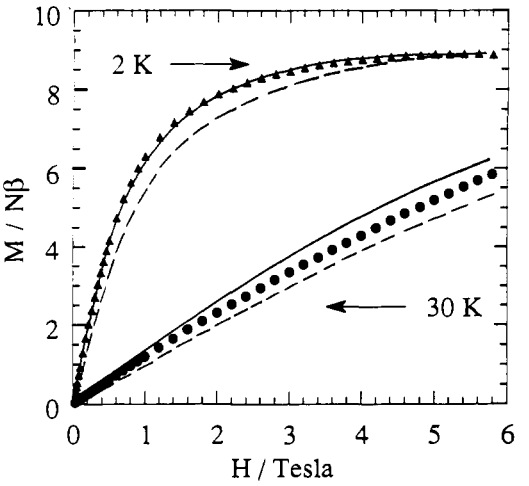

Figure 8. Field dependence of the magnetization for $[Gd_2Cu_4]$ at both 2 and 30 K. The full lines represent the Brillouin functions for two uncorrelated $S = {}^9/_2$ spins with $g = 1.99$, and the dotted lines represent the Brillouin functions for two local spins $S_{Gd} = {}^7/_2$ and four local spins $S_{Cu} = {}^1/_2$.

An alternative mechanism lies in the interaction between the 4f–3d ground configuration (GC) and the metal–metal charge-transfer configurations (CTC). The CTCs of lowest energy correspond to either the 3d → 4f or the 4f → 3d processes; both lead to a $S = 3$ excited-pair state. The transfer integrals β_{4f-3d}, however, are 0, such that the GC–CTC interaction cannot stabilize the low-lying $S = 3$ state. We are in the case where both Anderson's mechanism[35,36] ($\beta_{4f-3d}^2/U = 0$) and Kahn's mechanism[37,38] ($\beta_{4f-3d}S_{4f-3d} = 0$) are inoperative.

The CTC of energy immediately above is associated with the 3d → 5d process; an electron is transferred from the singly-occupied orbital centered on copper toward an empty orbital centered on gadolinium. Two excited states, $S = 3$ and $S = 4$, arise from this CTC. Due to Hund's rule, the latter is lower in energy than the former. The energy gap Δ between these two excited states is easily calculated as:

$$\Delta = E(S = 3)_{CTC} - E(S = 4)_{CTC} = 8k^0_{4f-5d} + \text{two-site ionic integrals} \quad (4)$$

where k^0_{4f-5d} is a mean one-site exchange integral which may be expressed as:

$$k^0_{4f-5d} = (1/7)\sum_{i=1}^{7}\langle 4f_i(1)5d(2)|1/r_{12}|4f_i(2)5d(1)\rangle \quad (5)$$

Let us define by U', the energy gap between the barycenters of the $S = 3$ and $S = 4$ pair states arising from the CTC, on the one hand, and the ground configuration on the other hand. U' represents the energy cost associated with the 3d → 5d electron transfer. Neglecting the two-site ionic integrals occurring in eq 4, the two coupling matrix elements $\langle(S = 3)_{GC}|H|(S = 3)_{CTC}\rangle$ and $\langle(S = 4)_{GC}|H|(S = 4)_{CTC}\rangle$ are equal to β_{5d-3d}. Thus, the GC–CTC interaction stabilizes the $S = 3$ and $S = 4$ low-lying pair states of $-\beta_{5d-3d}^2/(U' + \Delta/2)$ and $-\beta_{5d-3d}^2/(U' - \Delta/2)$, respectively. β_{5d-3d} is the transfer integral between a 5d-type orbital for gadolinium and the 3d-type magnetic orbital for copper. In contrast with β_{4f-3d}, β_{5d-3d} is far from being negligible. Indeed, the gadolinium 5d-type orbitals are very diffuse and may be delocalized toward the oxygen atoms surrounding the rare earth. The J_{GdCu} interaction parameter occurring in the spin Hamiltonian $-J_{GdCu}\mathbf{S}_{Gd}\cdot\mathbf{S}_{Cu}$ is equal to $[E(S = 3) - E(S = 4)]/4$, which leads to:

$$J_{GdCu} = \sum_{i=1}^{5}[\beta_{5d-3d}^2\Delta/(4U'^2 - \Delta^2)]_i \quad (6)$$

(38) Girerd, J. J.; Journaux, Y.; Kahn, O. *Chem. Phys. Lett.* **1981**, *82*, 534.

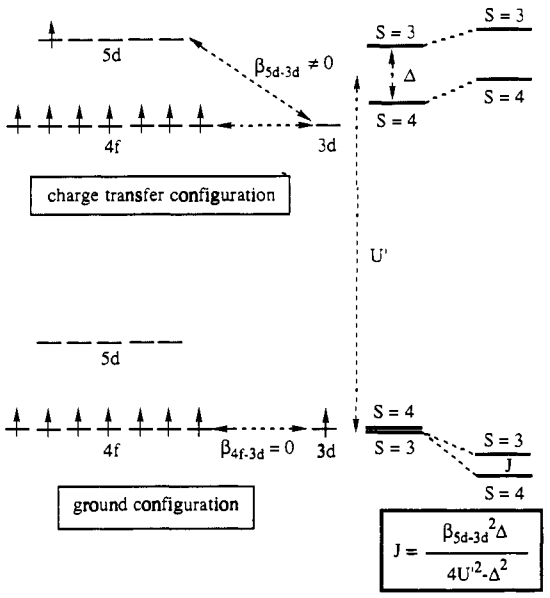

Figure 9. Schematic representation of the orbital mechanism explaining the ferromagnetic nature of the Gd(III)–Cu(II) interaction.

where the index i = 1–5 arises from the fact that the five 5d orbitals may be involved in the electron transfer. Equation 6 accounts for a ferromagnetic interaction. This mechanism is schematized in Figure 9.

It seemed to us worthwhile to determine the order of magnitude of J_{GdCu} in eq 6 and to compare it with the experimental value 6.0 cm^{-1}. In principle, the index i in eq 6 is attached to β_{5d-3d} as well as to Δ and U'. In fact, Δ and U' are deduced from atomic data and therefore can be viewed as mean values for the five 5d-type orbitals. Δ may be estimated from the $^7D - {}^9D$ energy gap between the two terms arising from the $4f^7 5d^1$ configuration of gadolinium(II). This gap has been found to be 8488 cm^{-1} by Callahan.[39] A very rough estimation of U' is given by the difference between the ionization potentials of Cu(II) and Gd(II), namely 120 000 cm^{-1}. The transfer integrals β_{5d-3d} are much more difficult to estimate. We used an Extended Hückel approach (detailed in the appendix) and obtained β_{5d-3d} values ranging from 1411 to 3838 cm^{-1}. The largest value is obtained with the 5d-type orbital of highest energy, which is the most delocalized toward the bridging oxygen atoms. J_{GdCu}, calculated from eq 6, is then equal to 4.8 cm^{-1}. The rusticity of the Extended Hückel method is well known, and the fairly good agreement with the experimentally determined J value is obviously somewhat fortuitous. This calculation, however, suggests that eq 6 gives not only the correct sign but also the correct order of magnitude for J_{GdCu}.

Discussion

The mechanism proposed to explain the ferromagnetic nature of the Gd(III)–Cu(II) interaction is in no way novel. It was introduced by Goodenough[40] as early as 1963 and was recently invoked by Tchougreeff[41] to justify the ferromagnetic ordering of decamethylferrocenium tetracyanoethenide, by Kinoshita and co-workers[42,43] to explain the intermolecular ferromagnetic coupling in (*p*-nitrophenyl)nitronyl nitroxide, and by Wieghardt, Girerd, and co-workers[44] to interpret the magnetic properties of μ-oxo manganese(III) compounds. The situation encountered in the Gd(III)Cu(II) compounds, however, has something unique. Let us show this specificity in quite a simple fashion for that which we consider a dissymmetric AB pair with the orbital pattern shown below, where a_1, and b_1 are natural orbitals[2,38] (they are not

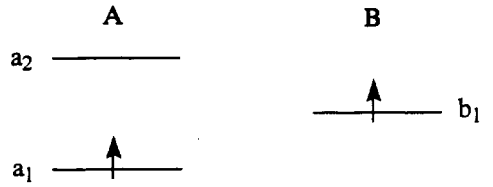

orthogonalized). The relative energies of the low-lying singlet and triplet states depend on three contributions arising from different mechanisms. (i) The Heitler–London interaction within the ground configuration $(a_1)^1(b_1)^1$, which leads to a singlet–triplet energy gap:

$$J_i \approx 2k_{11} + 4\beta_{11}S_{11} \quad (7)$$

where k_{11}, β_{11}, and S_{11} are the two-electron exchange, transfer, and overlap integrals, respectively, involving the a_1b_1 overlap density. In most cases the $4\beta_{11}S_{11}$ negative term dominates and the singlet state is the lowest. The triplet state becomes the lowest when the a_1 and b_1 orbitals are (quasi-) orthogonal. (ii) The interaction between GC and the first excited charge-transfer configurations $(a_1)^2$ and $(b_1)^2$. This contribution gives a further stabilization of the singlet state J_{ii}:

$$J_{ii} \approx -2\beta_{11}^2(1/U_A + 1/U_B) \quad (8)$$

where U_A and U_B are the energy costs associated with the $b_1 \rightarrow a_1$ and $a_1 \rightarrow b_1$ electron transfers, respectively. J_{ii} vanishes when a_1 and b_1 are orthogonal. (iii) The interaction between GC and the more excited charge-transfer configuration $(a_1)^1(a_2)^1$, which stabilizes the triplet state of a J_{iii} energy:

$$J_{iii} \approx 2\beta_{12}^2 k^0_{12}/U'^2 \quad (9)$$

where U' is the energy cost associated with this new electron transfer and k^0_{12} is the one-site exchange integral. J_{iii} in the general case is one order of magnitude smaller (in absolute value) than J_i and J_{ii} and is therefore masked by those two contributions. It is only when a_1 and a_2 are (quasi-) orthogonal that J_{iii} can be detected. But, if this is so, then the stabilization of the triplet state may be explained by the $2k_{11}$ term occurring in the Heitler–London contribution J_i; there is no need to invoke the J_{iii} term. The situation is different if a_1 is a rare-earth 4f orbital. In this case the overlap density a_1b_1 is 0 in any point of space and k_{11} vanishes. Only the J_{iii} term may account for a ferromagnetic interaction. In other words, the Gd(III)–Cu(II) case is ideal for investigating the effect of an electron transfer from a singly occupied orbital on a site toward an empty orbital on the other site. Of course, the ferromagnetic interaction cannot be very large since the stabilization of the high-spin state is given by a third order term, but there is nothing masking it.

It is worth pointing out that the mechanism developed above is largely in line with what had been briefly suggested by Gatteschi and co-workers, who attributed the ferromagnetic interaction to a "partial delocalization of the copper(II) unpaired electron toward the empty 6s orbital of Gd(III), which would force the seven f electrons of the rare earth to align parallel to this copper(II) electron on the basis of Hund's rule".[20] The 6s orbital, however, does not seem to be a good candidate for the electron transfer. Indeed, the lowest of the 5d levels for the Gd(II) ion is found to lie some 9000 cm^{-1} below the lowest 6s level.[39] Moreover, the k^0_{4f-6s} one-site exchange integral is smaller than k^0_{4f-5d}. Finally, in most of the Gd(III)–Cu(II) compounds we studied so far, including $[Gd_2Cu_4]$, the GdO_2Cu bridging network has a symmetry close to C_s with a pseudo-mirror plane perpendicular to this network, such that the β_{6s-3d} transfer integral is strongly reduced.

In other respects, Gatteschi defines its mechanism as a spin polarization effect. We think that this term "spin polarization"

(39) Callahan, W. R. *J. Opt. Soc. Am.* **1963**, *55*, 695.
(40) Goodenough, J. B. *Magnetism and Chemical Bond*; Interscience: New York, 1963.
(41) Tchougreeff, A. L. *J. Chem. Phys.* **1992**, *96*, 6026.
(42) Turek, P.; Nozawa, K.; Shiomi, D.; Awaga, K.; Inabe, T.; Maruyama, Y.; Kinoshita, M. *Chem. Phys. Lett.* **1991**, *180*, 327.
(43) Tamura, M.; Nakazawa, Y.; Shiomi, D.; Nozawa, K.; Hosokoshi, Y.; Ishikawa, M.; Takahashi, M.; Kinoshita, M. *Chem. Phys. Lett.* **1991**, *86*, 401.
(44) Hotzelmann, R.; Wieghardt, K.; Flörke, U.; Haupt, H. J.; Weatherburn, D. C.; Bonvoisin, J.; Blondin, G.; Girerd, J. J. *J. Am. Chem. Soc.* **1992**, *114*, 1681.

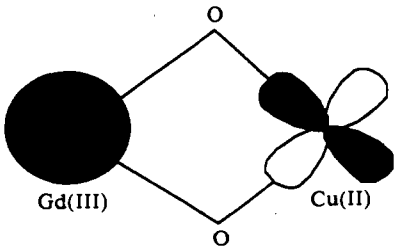

has a different meaning as far as the electronic structure of open-shell molecules is concerned, and thus it should be avoided here.

Conclusion

In this paper we first confirmed through accurate magnetic susceptibility and magnetization measurements that the Gd(III)–Cu(II) interaction was ferromagnetic, and then we proposed a mechanism to account for this behavior. The stabilization of the parallel spin state is attributed to the interaction between the Gd(III)Cu(II) ground configuration and the Gd(II)Cu(III) excited configuration arising from the 3d(Cu) → 5d(Gd) electron transfer. This mechanism is not novel. It was invoked for the first time by Goodenough.[4] However, most generally, it is masked by the Heitler–London-type interaction and/or the mixing of the ground configuration with the charge-transfer configuration of lowest energy, which are both one order of magnitude larger in absolute value. The Gd(III)–Cu(II) case is quite peculiar in this respect. Indeed, owing to the contraction of the 4f gadolinium orbitals, all 4f(Gd)–3d(Cu) overlap densities are expected to be negligibly small in any point of space. It follows that both the Heitler–London-type interaction and Anderson's GC–CTC mixing are inoperative. As a consequence of this, the mechanism requiring an electron transfer from a singly-occupied orbital on a site (3d(Cu) in the present case) to an empty orbital on the other site (5d(Gd) in the present case) is no longer hidden and even becomes preponderant. The efficiency of this mechanism in the Gd(III)–Cu(II) case lies on the values of the transfer integrals β_{5d-3d} on the one hand and the mean one-site exchange integral k^0_{4f-5d} on the other hand. The former integrals may be roughly estimated from an Extended Hückel calculation. Their rather large values are due to the diffuse character of the 5d rare earth orbitals. The value of the latter integral is deduced from the spectroscopic properties of the Gd(II) ion in the $4f^7 5d^1$ configuration.

This work, in our mind, is only the first step of a thorough investigation concerning the synthesis and the physical properties of 4f–3d compounds. The next step will deal with Ln(III)–Cu(II) species in which Ln(III) is a lanthanide(III) ion, the ground state of which possesses a first-order angular momentum. Quite original magnetic properties may be anticipated for such species. As a matter of fact, for the $4f^1$–$4f^6$ configurations of Ln(III), angular and spin momenta are antiparallel in the $^{(2S+1)}L_J$ free-ion ground state ($J = L - S$). A parallel alignment of the Ln(III) and Cu(II) spin momenta would lead to an antiparallel alignment of the angular momenta, i.e., to an overall antiferromagnetic interaction. On the other hand, for the $4f^8$–$4f^{13}$ configurations of Ln(III), angular and spin momenta are parallel in the ground state ($J = L + S$), and a parallel alignment of the Ln(III) and Cu(II) spin momenta would lead to a parallel alignment of the magnetic momenta, i.e., to an overall ferromagnetic interaction.

Of course, the actual situation may be more complicated owing to the partial splitting of the $^{2S+1}L_J$ free-ion ground state under the crystal field effect. Subsequent papers will be devoted to this problem.

Appendix

The calculation of the β_{5d-3d} transfer integrals was carried out as follows. We first constructed a simplified $O_8M(\mu\text{-}O_2)CuN_2$ network where M is a third-row metal ion with the $5d^1$ configuration (for instance Hf(III)) with the same environment as the rare earth in $[Ln_2Cu_4]$, the Cu(II) ion having also the same environment as in the actual compound. The next step consisted in determining the 3d- and 5d-type orbitals, centered on Cu and M, respectively. For that, we took advantage of an idea we proposed some time ago.[45] The 3d-type orbital is obtained as one of the two singly-occupied molecular orbitals in the triplet state after having contracted the coefficients of the 5d atomic orbitals for M in a way to prevent any interaction between M and its neighbors. Similarly, the 5d-type orbital for M is obtained as the other singly-occupied molecular orbital after having contracted the coefficients of the copper atomic orbitals. In the 3d → 5d electron transfer, it is obvious that the 3d orbital of interest is that pointing from the metal toward the four nearest neighbors in the basal plane ($3d_{x^2-y^2}$). On the other hand, the electron transfer may occur to any of the 5d orbitals, not only that of lowest energy. That is why we determined the five 5d-type orbitals. The third step consisted in calculating the five β_{5d-3d} integrals from the 3d- and 5d-type eigenvectors, the overlap matrix and the usual Mulliken approximation for the $\langle\phi_i|H|\phi_j\rangle$ transfer integral between ϕ_i and ϕ_j atomic orbitals: $\langle\phi_i|H|\phi_j\rangle = (K/2)\langle\phi_i|\phi_j\rangle(\langle\phi_i|H|\phi_i\rangle + \langle\phi_j|H|\phi_j\rangle)$ K is the Wolfsberg–Helmholz coefficient, generally taken to be equal to 1.75. All the calculations were performed in the framework of the Extended Hückel formalism without charge iteration. The basis set was made of the 5d, 6s, and 6p orbitals for M, the 3d, 4s, and 4p orbitals for Cu, the 2s and 2p orbitals for the bridging oxygens, and the 2s orbitals standing for the lone pairs for the terminal nitrogens and oxygens. The parameters were the following: M, −13.1 eV (4.762 and 1.938), −10.1 eV (2.280), −6.86 (2.240); Cu, −14.0 eV (5.950 and 2.300), −11.4 eV (2.200), −6.06 eV (2.200); bridging O, −32.3 eV (2.275), −14.8 eV (2.225); terminal O, −20.6 eV (2.275); terminal N, −16.55 eV (1.950). The Wolfsberg–Helmholz K parameter was taken as 1.75.

The $|\beta_{5d-3d}|$ absolute values of the transfer integrals, ranked according to the increasing energies of the 5d-type orbitals, were found to be 1411, 2338, 1790, 2709, and 3838 cm^{-1}.

Supplementary Material Available: Listing of experimental crystallographic data, atomic parameters, interatomic distances and angles within the ligands $(fsaaep)^{2-}$ and the nitrato groups (Tables SI–SVIII); view of the copper and praseodymium coordination polyhedra (Figures S1 and S2) (17 pages); tables of calculated and observed structure factors (25 pages). Ordering information is given on any current masthead page.

(45) Gillon, B.; Cavata, C.; Schweiss, P.; Journaux, Y.; Kahn, O.; Schneider, D. *J. Am. Chem. Soc.* **1989**, *111*, 7124.
(46) Supplementary Material.